The structural basis for specificity of substrate and recruitment peptides for cyclin-dependent kinases

Nick R. Brown*†, Martin E. M. Noble*†, Jane A. Endicott* and Louise N. Johnson*‡

*Laboratory of Molecular Biophysics and Oxford Centre for Molecular Sciences, Department of Biochemistry, University of Oxford, Rex Richards Building, South Parks Road, Oxford OX1 3QU, UK

‡email: louise@biop.ox.ac.uk

†These authors contributed equally to this work

Progression through the eukaryotic cell cycle is driven by the orderly activation of cyclin-dependent kinases (CDKs). For activity, CDKs require association with a cyclin and phosphorylation by a separate protein kinase at a conserved threonine residue (T160 in CDK2). Here we present the structure of a complex consisting of phosphorylated CDK2 and cyclin A together with an optimal peptide substrate, HHASPRK. This structure provides an explanation for the specificity of CDK2 towards the proline that follows the phosphorylatable serine of the substrate peptide, and the requirement for the basic residue in the P+3 position of the substrate. We also present the structure of phosphorylated CDK2 plus cyclin A3 in complex with residues 658–668 from the CDK2 substrate p107. These residues include the RXL motif required to target p107 to cyclins. This structure explains the specificity of the RXL motif for cyclins.

Eukaryotic cells proceed through the cell division cycle in a strictly ordered fashion. Cell-cycle transitions are coordinated in large part through the action of a family of CDKs. For activity, CDKs require association with a cyclin and phosphorylation by a separate protein kinase at a conserved threonine (T160 in CDK2)[1]. Concentrations of the cyclins oscillate during the cell cycle and are regulated by successive rounds of transcription followed by ubiquitin-mediated proteolysis, which results in abrupt inactivation of the associated CDK. Further cellular controls are provided by the binding of CDK inhibitors, such as $p27^{KIP1}$, and by inhibitory phosphorylation on a tyrosine residue (Y15 in CDK2) close to the ATP-binding site. Cyclins are important for ensuring that CDKs are activated at the correct points in the cell cycle, targeted to the correct substrates and localized to the correct subcellular regions. Each phase of the cell cycle is characterized by the expression of different CDK–cyclin complexes that phosphorylate and regulate downstream substrates. In vertebrates, CDK4–cyclin D is active throughout G1 phase, CDK2–cyclin E at the G1/S boundary, CDK2–cyclin A during S phase, and CDK1–cyclin A and CDK1–cyclin B during the transition from G2 to M phase.

Despite recent advances in studying CDK structures[2–6], there are no data available about the key events required for substrate recognition and targeting. The canonical amino-acid sequence in substrates that is recognized by CDKs is S/TPXK/R, where S is the phosphorylatable serine and X is any amino acid[7–11]. Targeting of CDK substrates is also guided by a remote binding site present on the cyclin molecule. Substrates containing the motif RXL[12–17] bind to this site, and peptides containing this motif inhibit catalysis, a property that has led to the design of antineoplastic agents[18]. Identification of *in vivo* substrates for members of the CDK family, phosphorylation by which is demonstrably and directly relevant to cell-cycle progression, is an ongoing process. The cyclin also plays a part in substrate specificity, as shown by the fact that, when in complex with cyclin A, CDK2 has a broad range of substrates, some of which are consistent with its role in promoting DNA replication throughout S phase[19]; however, CDK2 is more selective when in complex with cyclin E[11,20–22], and the CDK2–cyclin E complex shares just a few of the substrates of CDK2–cyclin A complexes, such as the retinoblastoma protein (pRb) and $p27^{KIP1}$.

The CDK2 molecule, in common with other protein kinases, comprises an amino-terminal lobe that is rich in β-sheet and has just one major helix, the C (PSTAIRE) helix, together with a larger, mostly α-helical carboxy-terminal lobe which contains the activation segment. The activation segment spans residues D145 (the DFG motif) to E172 (the APE motif) and includes the phosphorylated T160 residue (Fig. 1a, b). Association with cyclin A results in rearrangements in the structure of inactive unphosphorylated CDK2 in the region of the C-helix, the activation segment and in the relative orientation of the N- and C-terminal lobes, producing a conformation in which the substrate site for ATP is correctly formed[2,4]. The cyclin, however, undergoes no conformational changes between its free, bound and fully active states[3]. Full activity of the CDK2–cyclin A complex is generated by phosphorylation of CDK2 residue T160, which results in further changes in the activation segment[5].

Results

Binding of a substrate peptide. We determined, at 2.2 Å resolution, the crystal structure of a complex consisting of CDK2 phosphorylated at T160, cyclin A3 and a CDK2 substrate peptide (phospho-CDK2–cyclin A3–peptide complex; see Methods and Table 1; 'cyclin A3' is defined in Methods). The substrate peptide (HHASPRK, derived from the optimal substrate peptide of ref. 7) binds in an extended conformation across the catalytic site on the surface of the kinase, contacting only the C-terminal lobe of CDK2, especially the activation segment (Fig. 1a, c).

The specificity of CDK2 for a proline at the P+1 position, following the phosphorylatable serine, of the substrate is explained by the substrate's contacts with, and conformation of, the activation segment, which forms a suitably shaped pocket to accept the proline (Fig. 2a). In both the uncomplexed and the peptide-complexed phospho-CDK2–cyclin A3 structures, the activation-segment residue V164 has an unusual left-handed conformation ($\phi = 72.5°$, $\psi = 130.8°$) that results in the carbonyl oxygen atom being directed away from the substrate. This unfavourable conformation is compensated by the existence of hydrogen bonds from the main-chain carbonyl oxygen of V164 to the NH_2 group of R169, and from the main-chain nitrogen of V164 to the carbonyl oxygen of R126 from the catalytic loop. Binding of any residue except proline at the P+1

site would be unfavourable because of an uncompensated hydrogen bond from the substrate's main-chain nitrogen. The different conformation of the activation segment in the unphosphorylated CDK2–cyclin A3 complex is shown in Fig. 2a. This different conformation does not affect V164 but does affect V163, whose main-chain carbonyl oxygen blocks the P+1 site in the unphosphorylated complex, thus indicating the importance of the change in conformation of the activation segment after phosphorylation for substrate binding (Fig. 2a). Phosphorylation of T160 results in an increase in activity of CDK2–cyclin A from a basal 0.3% to 100% (ref. 5).

The arginine at the P+2 site of the substrate peptide makes no contacts with the protein and is directed to the solvent. Comparative studies with a peptide library have shown a preference for arginine, lysine or methionine at the P+2 site[9], indicating that, despite the lack of specific contacts, a long aliphatic amino acid or a positively charged residue at the P+2 position contributes to efficiency of phosphorylation of the peptide substrate. A major interaction occurs with the lysine in the P+3 position that explains the specificity for basic residues at this position. The lysine side chain is well located and the sidechain atoms have B-factors below the average for the peptide. The lysine is hydrogen-bonded to the T160 phosphate and to the main-chain oxygen of residue I270 on cyclin A3 (Fig. 2a). The contact to I270 on cyclin A3 is the only contact from the substrate to the cyclin. The surface presented by the binary complex indicates that further residues of the substrate would contact sites formed predominantly by cyclin A (Fig. 1c).

The conformation of the peptide explains the specificity for proline at P+1 and lysine at P+3. The restricted conformational angles of the *trans* proline residue ($\phi = -62.9°$, $\psi = 135.0°$) direct the side chain of the P+2 site to the solvent and allow the side chain of the P+3 site to be directed towards the T160 phosphate. In the structure of the phosphorylase kinase (PhK) complex with peptide[23], the peptide binds with an extended conformation at the P+1 position ($\phi = -145.5°$, $\psi = 166.5°$) and the side chain of the P+2 site is directed towards E182, the residue corresponding to T160 phosphate in CDK2 (Fig. 2b). Residue G185 in PhK (equivalent to V164 in CDK2) has conventional ϕ and ψ angles and its main-chain oxygen

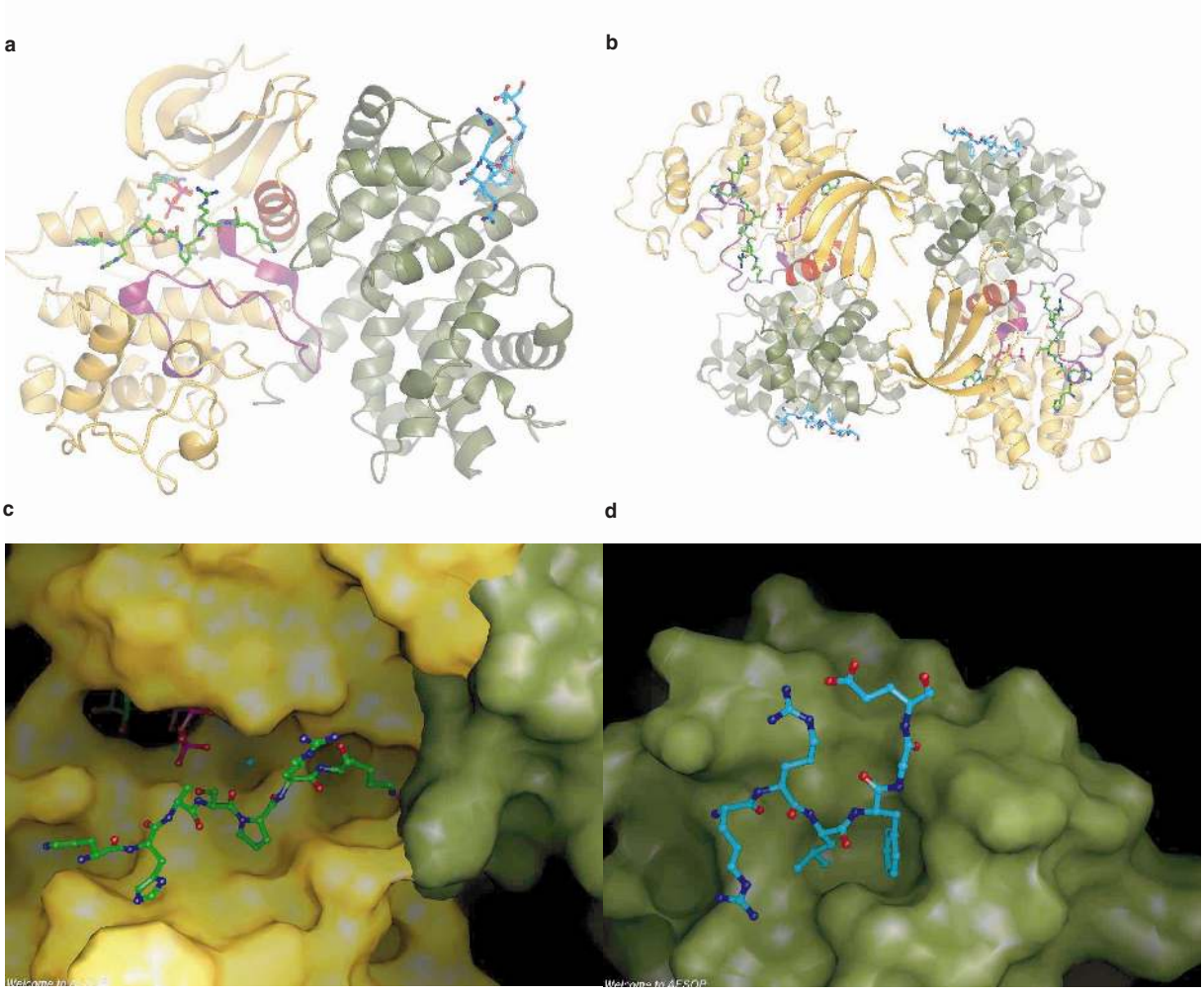

Figure 1 **The location of the peptide-binding sites on phospho-CDK2–cyclin A3 complex.** CDK2 is shown in yellow with the C (PSTAIRE) helix in red and the activation segment in magenta. Cyclin A3 is shown in khaki. **a**, Conventional view of the CDK2–cyclin A3 complex, also showing the peptide substrate (green ball-and-stick diagram) and the recruitment peptide (cyan ball-and-stick diagram). Note that the structures of the two phospho-CDK2–cyclin A3–peptide complexes were determined separately. **b**, Dimeric phospho-CDK2–cyclin A3 complexes. The phospho-CDK2–cyclin A3–peptide complexes in the crystal formed dimers, with the two complexes related by a non-crystallographic two-fold axis, in an arrangement similar to that of the phospho-CDK2–cyclin A3 crystal (coordinates 1JST)[5], which crystallized in a different space group to the peptide complexes. The contacts across the dimer interface are between the β-sheet region of CDK2 (end of β2 and start of β3) and the groove between helices in cyclin A3 (helices α3 and α5). **c**, Surface representation of the substrate-peptide-binding pocket of CDK2, showing the site for proline at P+1 and the proximity of lysine at P+3 to cyclin A3. **d**, Surface representation of the recruitment-peptide complex. Diagrams generated in AESOP (M.E.M.N., unpublished observations).

participates in an antiparallel β-sheet with the substrate peptide, an arrangement that would not be possible with a proline residue in the peptide substrate. In PhK there is a preference for large nonpolar groups in the P+1 position, and the phenylalanine side chain is directed deep into the loop created by the activation segment. In CDK2, location of a large residue at P+1 is excluded by the large side chain of R169, whereas the equivalent residue in PhK is the smaller residue V190.

In the phospho-CDK2–cyclin A3–peptide structure, the substrate peptide makes fewer interactions with phospho-CDK2–cyclin A3 on the N-terminal side of the phosphorylatable serine. Histidine at position P–3 contacts W167, a residue from the activation segment, while the histidine at position P–2 is external and makes one hydrogen bond from NE2 to the main chain of G205, the glycine of the conserved CDK motif GDSEID (Fig. 2a). Sites P–3 to P–1 appear relatively nonspecific, with scope for accommodation of a variety of residues, as observed in CDK2 substrates. Histidine occurs in the P–3 position in SKP2 and in the P–2 position in pp60$^{c\text{-}Src}$. Holmes and Solomon observed no preference for amino acids in the P–1 position[9].

We used the inactive ATP analogue AMPPNP in our crystallization procedure; AMPPNP binds at the interface between the two lobes of the kinase, contacting mostly the N-terminal lobe. The serine at the P0 position of the peptide is directed towards the γ-phosphate of the AMPPNP. In contrast to other CDK2 structures[2,4,5], the three phosphate groups of the AMPPNP are localized in a conformation that permits phospho-transfer to the peptide serine residue (Fig. 2c). As observed previously for CDK2, there is only one bound magnesium ion (Mg^{2+}) in the structure. The Mg^{2+} is bound in octahedral coordination and chelates the α- and γ-phosphates. The substrate peptide serine at P0 is hydrogen-bonded with the conserved catalytic aspartate, D127, and the conserved lysine, K129. The serine side chain is positioned so that, when in complex with ATP, its lone-pair electrons are directed in-line to the βγ-bridging oxygen of the bound ATP through the γ-phosphorous atom. D127 is poised to assist catalysis by both orientational effects and general base/general acid catalysis, while K129 may assist in stabilizing the negative charge in the transition state, as proposed for PhK[24]. Contacts to the T160 phosphate involve R50 from the C-helix and R126 and R150 from the start of the activation segment. The arginine side chains also make hydrogen bonds across to the main-chain oxygen atoms of residues F267 and E268 on the cyclin A3 molecule (Fig. 2c). Binding of peptide substrate does not perturb these contacts.

Binding of a recruitment peptide. We also determined the crystal structure of a complex consisting of phospho-CDK2–cyclin A3 together with the p107-derived RXL-containing recruitment peptide. This structure showed binding of the recruitment peptide at a hydrophobic site on the surface of the cyclin (Fig. 1a, d). This site had previously been predicted to be a binding site on the basis of the conservation of exposed residues in cyclins A, B and E[3] and was identified in the p27^{KIP1}–phospho-CDK2–cyclin A3 complex[25]. Of the 11 residues in the peptide used (p107 residues 558–668, sequence RRLFGEDPPKE), only the first six were located in the structure. These amino acids were assigned the same residue numbers as the equivalent residues in p27^{KIP1}. The conformations of the cyclin A3 molecule and phospho-CDK2 do not change on binding the recruitment peptide. The peptide-binding site in cyclin A3 is composed of residues M210, I213, W217 and E220 from four successive turns of the α1 helix, and residues L253 and Q254 from the α3 helix of the cyclin-box fold. These residues are conserved in cyclins A, B, D and E, with the exceptions of E220, which is glutamine in cyclin B, and L213, which is valine in cyclin D.

In the recruitment-peptide complex (Fig. 3a), the side chain of R30 forms ion pairs with E220 of cyclin A3, explaining the specificity for the arginine of the RXL motif. R31 is largely external but it makes an ion pair with the glutamate residue of the peptide four residues away. L32 makes a hydrogen bond from its main-chain nitrogen to cyclin A3 residue Q254 and makes extensive van der Waals contacts with the side chain of Q254 and with W217. The hydrophobic site is shielded from solvent by the neighbouring peptide residues L32 and F33. F33 makes van der Waals contacts to cyclin residues M210, I213 and L253. In total there are 23 van der Waals interactions between the phenylalanine side chain and these residues, indicating an extensive hydrophobic interaction. G34 and E35 have conventional extended main-chain conformations that allow the side chain of E35 to form an ion pair with R31.

Comparison of the p27^{KIP1} and the recruitment-peptide complexes shows identical interactions between cyclin A3 and the RXLF motifs (Fig. 3b). The major difference occurs with the subsequent residues; in p27^{KIP1}, the glycine has φ and ψ angles that other amino acids cannot adopt and, in conjunction with the following proline at position 35, allows the p27^{KIP1} peptide to exit from the cyclin groove. The turn between residues 31 and 34 in p27^{KIP1} is stabilized

Table 1 Crystallographic data and refinement statistics

	Phospho-CDK2–cyclin A3–substrate peptide	Phospho-CDK2–cyclin A3–recruitment peptide
Data collection		
Cell dimensions (Å) (space group $P2_12_12$)	152.6, 163.7, 73.3	151.7 165.1 73.4
Maximal resolution (Å)	2.2	2.1
Observations	146,344	189,383
Unique reflections (Completeness (%))	51,615 (95.4)	67,852 (98.5)
R_{merge}*	0.12	0.08
Mean $I/\sigma(I)$	8.1	4.2
Highest resolution bin (Å)	2.32–2.20	2.21–2.10
Completeness (%)	95.4	98.5
R_{merge}*	0.51	0.32
Mean $I/\sigma(I)$	2.5	2.0
Refinement		
Protein atoms	9,062	9,052
Residues	1,124	1,122
Other atoms	827 (62 AMPPNP, 2 Mg, 763 H_2O)	1,065 (46 AMPPNP,1,019 H_2O)
Resolution range (Å)	20.0–2.2	20.0–2.1
R_{conv}†	0.22	0.22
R_{free}‡	0.28	0.27
Mean protein main-chain temperature factor (Å^2)	34.3	26.7
Mean peptide temperature factor (Å^2)	53.3	41.2
r.m.s.d. bond lengths (Å)	0.019	0.015
r.m.s.d. bond angles (°)	2.7	2.1

* $R_{merge} = \frac{\sum_h \sum_j |I_{h,j} - \bar{I}_h|}{\sum_h \sum_j |I_{h,j}|}$

where $I_{h,j}$ is the intensity of the jth observation of unique reflection h.

† $R_{conv} = \frac{\sum_h ||Fo_h| - |Fc_h||}{\sum_h |Fo_h|}$

where Fo_h and Fc_h are the observed and calculated structure factor amplitudes for reflection h.
‡ R_{free} is equivalent to R_{conv}, but is calculated using a 5% disjoint set of reflections excluded from the least-squares refinement stages.
r.m.s.d., root mean square deviation.

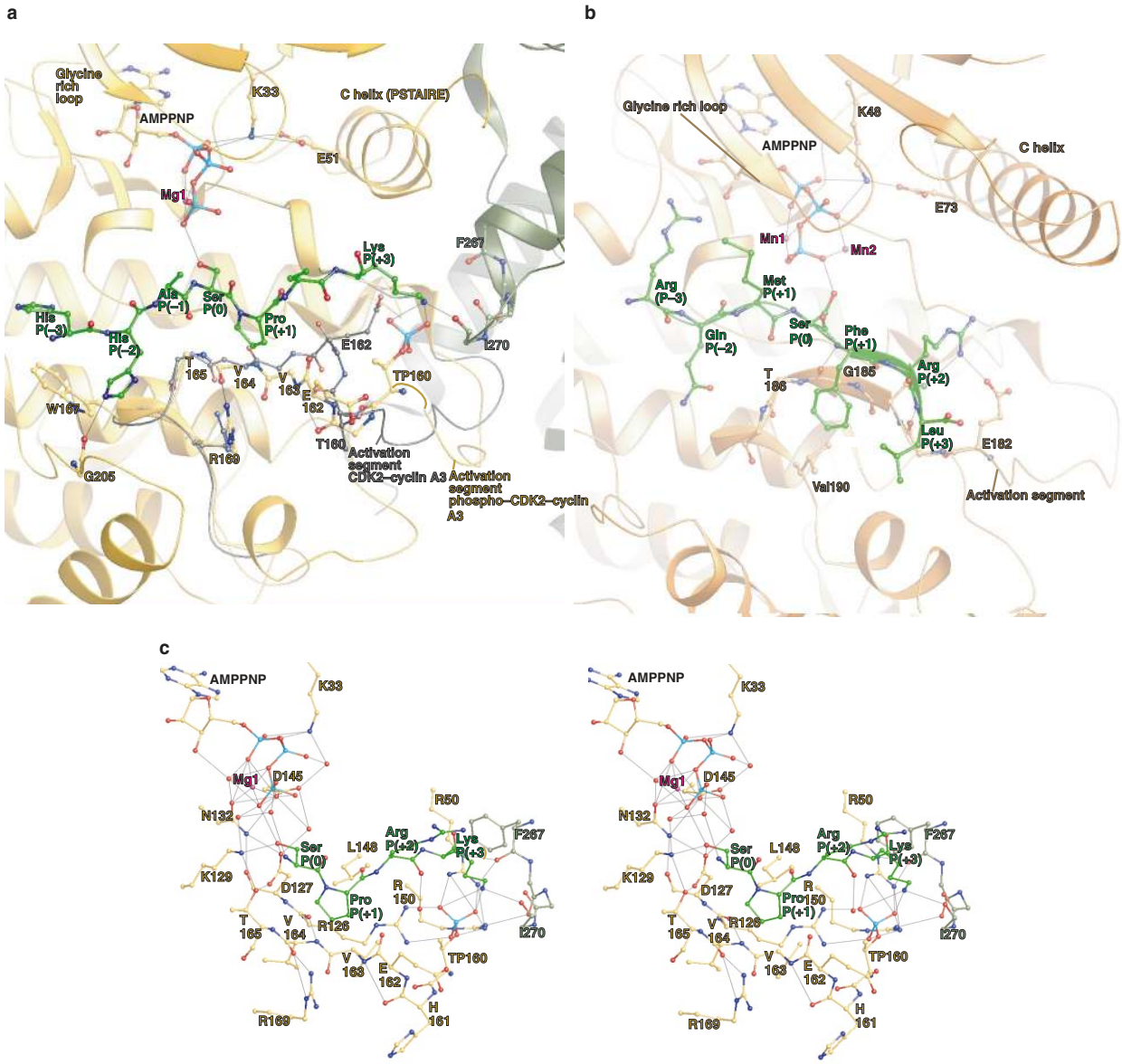

Figure 2 **Contacts between CDK2 and the substrate peptide. a**, Interactions of the substrate peptide with phospho-CDK2–cyclin A3 in the region of the activation segment and other selected residues. The colour scheme is as in Fig. 1, except that all of CDK2 is in yellow. The activation segment of the partially active CDK2–cyclin A3 complex is shown in grey. For further details, see text. **b**, A similar view of PhK in complex with a substrate peptide. **c**, Stereo diagram showing details of the interaction of the peptide substrate in the vicinity of the P0 to P+3 sites with AMPPNP and phosphorylated T160 in the phospho-CDK2–cyclinA3 complex. Contacts from the phospho-CDK2–cyclin A3 complex to the proline at P+1 of the substrate peptide include main-chain atoms from residues 162–165, I148 and the aliphatic side chain of E162. On forming the peptide-substrate complex there is only one significant conformational change in phospho-CDK2–cyclin A3. The interchange of the positions of H161 from internal to external and of E162 from external to internal allows the aliphatic component of the glutamate side chain to contribute van der Waals interactions to the P+1 proline.

by two internal hydrogen bonds between the side chain of N31 and the main-chain nitrogen and oxygen atoms of G34. In the recruitment-peptide complex, the internal ion pair between the side chains of R31 and E35 has a similar role.

In kinase assays, the recruitment peptide of p107 inhibited the phosphorylation of a substrate composed of glutathione-*S*-transferase (GST) fused with the C-terminal residues of pRb (residues 792–928, which include a KPLKKL recruitment motif known to be necessary for efficient phosphorylation of upstream sites[17]) (Fig. 4). In contrast, the p107 recruitment peptide had no effect on the phosphorylation of histone H1, a substrate that does not contain a recruitment site.

Discussion

The results with the phospho–CDK2–cyclin A3–substrate complex provide an explanation for the specificity for proline in P+1 and a basic residue in P+3. Mitogen-activated protein kinase (MAPK) also shows specificity towards a proline residue in the P+1 position. In the structure of doubly phosphorylated MAPK[26], the activation segment has an almost identical conformation to the activation segment of the phospho-CDK2–cyclin A3–substrate complex, including the unusual ϕ and ψ angles for residue A187, the residue corresponding to V164 in CDK2. Thus the strained conformation of the activation segment in this region, coupled with the shape of the binding pocket, may also provide an explanation for the specif-

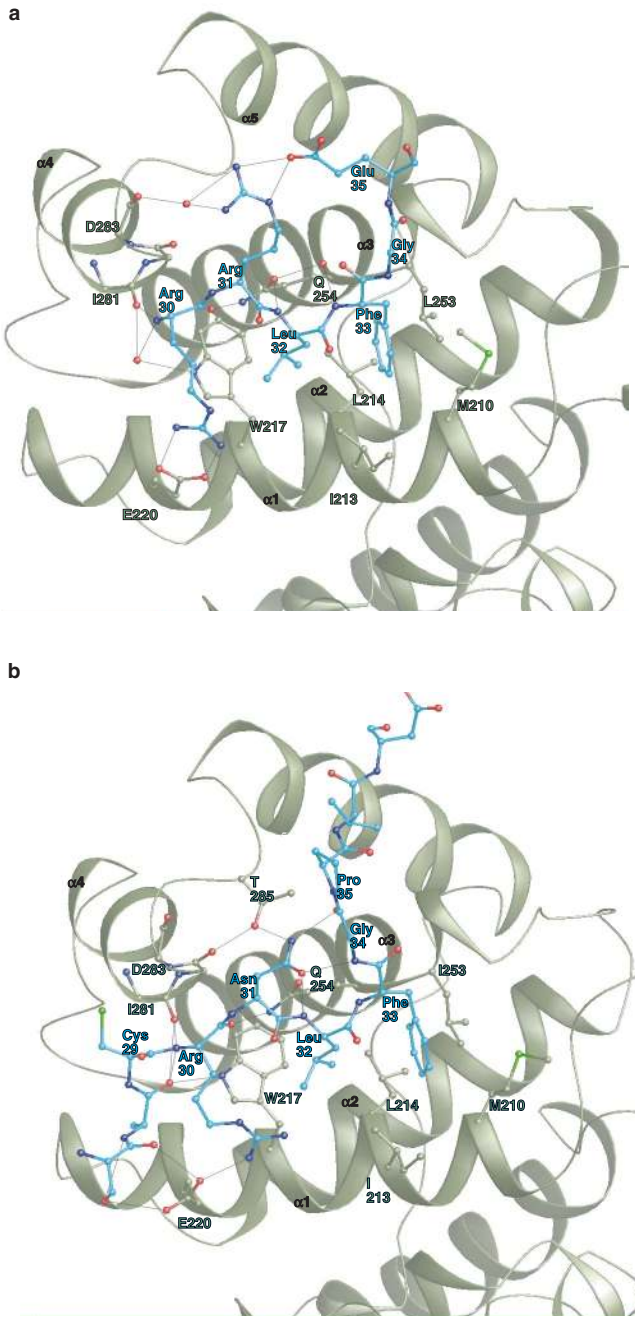

Figure 3 **The recruitment-peptide-binding site of the phospho-CDK2–cyclin A3 complex. a**, Diagram showing residues RRLFGE from the recruitment peptide of p107 bound at the hydrophobic site on cyclin A3, making contacts with residues from successive turns of the α1 and α3 helices. The view, which is rotated ~90° from that shown in Fig. 2, shows the complete fold of the cyclin box. **b**, Similar view of the equivalent residues from the phospho-CDK2–cyclin A3–$p27^{KIP1}$ complex (coordinates IJSU from the PDB[25]).

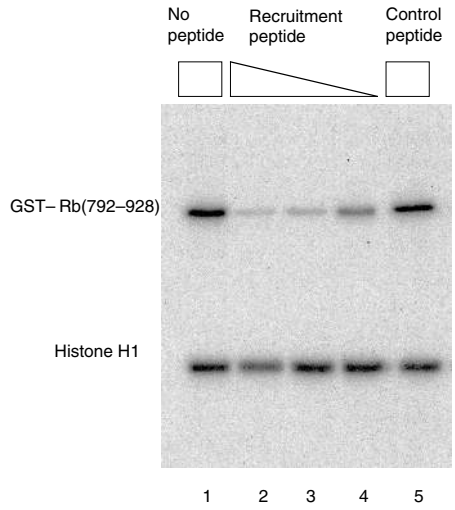

Figure 4 **The recruitment peptide inhibits the phosphorylation of GST–pRb (residues 792–928) but not phosphorylation of histone H1.** 1.6 nM phospho-CDK2–cyclin A3 was pre-incubated on ice for 5 min in the absence of peptide (lane 1), with 2,000 μM, 200 μM and 2 μM recruitment peptide (lanes 2–4) or with 2,000 μM control peptide (lane 5) before the addition of 2.5 μM GST–Rb (residues 792–928) or 3 μM histone H1, plus 0.1 mM ATP, 1 μCi [^{32}P]ATP, 5 mM $MgCl_2$ and 50 mM Tris/HCl, pH 7.5, in a final volume of 10 μl. The reaction was allowed to proceed for 10 min on ice and the samples were analysed by SDS–PAGE and autoradiography. The control peptide was YEYRHVMLPKAMLK (derived from residues 35–48 of *Schizosaccharomyces pombe* $p13^{suc1}$).

icity of MAPK for proline in the P+1 position, as predicted[26]. The participation of the T160 phosphate in substrate recognition at the P+3 site has been anticipated by J. Holmes and M.J. Solomon (unpublished observations, cited in ref. 27), who found that whereas phosphorylation of the substrate SPRA by phospho-CDK2–cyclin A is greatly reduced relative to the phosphorylation of an optimal substrate, SPRK, the unphosphorylated CDK2–cyclin A complex phosphorylated both substrates with diminished but nearly equivalent efficiency. Alternative suggestions for the specificity of the basic group in the P+3 position[5] that invoked a cluster of acidic residues on the surface of CDK2, and suggestions (from computer simulations and mutational studies) of an alternative binding mode for a substrate of CDK5 ref. 28, are not substantiated by our results.

The structure of the recruitment-peptide complex confirms the commonality of binding modes between RXL motifs involved in the recruitment of either a substrate (p107) or an inhibitor ($p27^{KIP1}$). It appears that residues located C-terminally to the core RXLF motif of p107 have a limited function in recognition, as they cannot be seen in our electron density. The degenerate nature of the RXL signal raises the question of how specificity is achieved. Interactions between residues flanking the leucine and phenylalanine residues, seen in both the recruitment-peptide structure and that of $p27^{KIP1}$–CDK2–cyclin A, show that the RXLF motif is restrained in a conformation that favours interaction with cyclin A3. These considerations suggest that conformational restraints add an additional component for specificity.

Despite the inhibitory potency of RXL peptides, the connection between the RXL-binding site and the catalytic binding site is not understood. Within the CDK2–cyclin A3 complex, the shortest distance between the serine of the substrate peptide and the arginine of the RXL recruitment peptide motif is 40 Å. However, as is apparent from Fig. 1b, the path would need to take a route around the CDK2–cyclin A3 and would be longer than 40 Å. Alternatively, with the dimeric CDK2–cyclin A3 observed in the crystal structures, there could be a connection (distance 53 Å) from the substrate of one subunit to the recruitment site of the other subunit. But although dimers are observed in the crystals (in at least three different crystal forms), there is no evidence for the dimeric association of CDK2–cyclin A in cells. Examination of substrates of CDKs shows no fixed relationship between sites of phosphorylation and those of recruitment, and it may be that there is no fixed route for communication.

The experimental results of Schulman *et al.*[16] have indicated that the primary role of the RXL-recognition motif may be to increase the local concentration of substrate relative to the catalytic site. From our structures we cannot address the question of whether or not the two recognition events occur simultaneously, but it is noteworthy that the involvement of two binding sites in substrate selection allows for the observed occurrence of shared and distinct phosphorylation sites between different CDK–cyclin pairs. □

Methods

Bacterial expression and purification of human phospho-CDK2–cyclin A3.

CDK2 phosphorylated at T160 was produced in *Escherichia coli* by coexpression of human GST–CDK2 and *S. cerevisiae* GST–Cak1 (Cak1 is also called Civ1). *E. coli* strain B834 (DE3) pLysS, transformed with the coexpression plasmid (details of which will be described elsewhere; N. Hanlon, N.R.B., J. Tucker and D. Barford, unpublished observations), were grown in LB medium supplemented with 50 μg ml^{-1} ampicillin to an optical density of 0.9 at 37 °C and then at 20 °C for 1 h, before induction with 80 μM isopropyl-β-D-thiogalactoside (IPTG) and further incubation for 20–24 h at 20 °C. Collected cells were resuspended in HEPES-buffered saline (HBS) containing protease inhibitors (10 mM HEPES, pH 7.4, 135 mM NaCl, 3 mM EDTA, 0.01% (*v*/*v*) monothioglycerol, and 0.01 % (*w*/*v*) sodium azide containing 0.1 mM phenylmethylsulphonyl fluoride (PMSF), 0.7 μg ml^{-1} pepstatin A and 0.5 μg ml^{-1} leupeptin) and stored at –20 °C.

Human cyclin A3 complementary DNA was generated by the polymerase chain reaction (PCR) using a Δ47 cyclin A expression plasmid (a gift from M. Dorée) as a template. cyclin A3 (residues 174–432) can activate CDK2 but lacks the destruction box that targets the cyclin for ubiquitination and destruction[29]. The PCR cloning strategy changed residue N173 to the start methionine. This sequence was inserted into pET21d and expressed as an untagged polypeptide. Transformed B834 (DE3) pLysS cells, at an optical density of 0.7, were induced with 100 mM IPTG at 37 °C for 30 min and further incubated at 30 °C for 3–4 h. Cells were stored as above.

GST–3C-protease (a gift from J. Heath) and GST–pRb (residues 792–928) (a gift from T. Boyle) were expressed using pGEX-2T recombinant plasmids. Both were induced at 25 °C with 0.1 mM IPTG for 20 h. GST–3C-protease and GST–pRb (residues 792–928) were purified using glutathione–Sepharose chromatography.

Cells coexpressing GST–CDK2 and GST–Cak1 were thawed and sonicated on ice. The clarified lysate was applied to a glutathione–Sepharose column (Amersham) equilibrated in HBS and washed with the same buffer. A clarified lysate from thawed and sonicated cyclin-A3-expressing cells was applied to the washed column. GST–phospho-CDK2–cyclin A3 complex was eluted with freshly prepared 20 mM glutathione in HBS and subjected to GST–3C-protease digestion (1/30 *w*/*w*, 16 h, 4 °C). Phospho-T160-CDK2–cyclin A3 was further purified from GST and from GST–Cak1 (where the fusion protein does not contain a 3C-protease-sensitive site) by gel filtration (Superdex 75 HR 26/ 60) and a second glutathione–Sepharose column. Typical yields of phospho-CDK2–cyclin A3 were 10–15 mg from 1 l and 1.5 l of CDK2 and cyclin A3 cultures, respectively.

Co-crystallization of synthetic peptides with phosphorylated binary complex.

Phospho-CDK2–cyclin A3 was concentrated to 10–15 mg ml^{-1} in a Centricon-10 (Millipore); the solution was clarified by centrifugation and mixed with 1 mM (final concentration) peptide and 1 mM (final concentration) adenylyl imidodiphosphate (AMPPNP). Crystallization trials were done at 4 °C using the vapour diffusion technique with 2 μl sitting drops. The crystals obtained in the presence of the recruitment peptide (RRLFGEDPPKE) had a plate-like appearance and the thickest examples (up to 40 μm) were grown from 1.0–1.1 M Li_2SO_4 plus 100 mM HEPES, pH 7.0. The crystals obtained in the presence of the substrate peptide (HHASPRK) had the same morphology and the largest were grown from 0.9–1.0 M Li_2SO_4 plus 100 mM HEPES, pH 7.0.

Phospho-CDK2–cyclin A3 crystals grown in the presence of substrate peptide showed no binding of peptide in a subsequent difference Fourier map at 2.1 Å resolution. We considered that the high concentration of Li_2SO_4 might have prevented binding by reducing charge–charge interactions. Accordingly, crystals were transferred to a more nonpolar medium of polyethylene glycol with guidance from protocols described in ref. 30. Phospho-CDK2–cyclin A3 crystals grown in the presence of 1 mM substrate peptide were transferred to a solution containing 35% PEG 8000, 100 mM HEPES, pH 7.0, 10 mM peptide, 3 mM AMPPNP and 5 mM $MgCl_2$ for 64 h. Crystals of both peptide complexes were soaked for 1 min in the crystallization solution to which 25% glycerol had been added for cryoprotection.

Determination of crystal structures.

X-ray data for the substrate peptide were collected at the X-ray diffraction beam line, Elettra, Trieste, using a 345-mm MAR imaging plate detector. Data for the recruitment peptide were collected on EH3 of ID14 at the ESRF, Grenoble. The recruitment-peptide structure was solved by molecular replacement in the AMoRe[31], package starting with the coordinates of 1JST from the PDB[5]. The translation function was used to identify the space group as $P2_12_12$, with two phosphorylated binary complexes in the asymmetric unit, and the non-crystallographic two-fold axis parallel with *c*. The structure was subjected to rigid-body refinement in REFMAC[32] using data of increasing resolution and rigid bodies of decreasing size. SIGMA-A-weighted[33] $2F_o–F_c$ and $F_o–F_c$ maps were used to guide rebuilding of the structure in program O (ref. 34) and fitting of the peptide into clear electron density. Subsequent refinement involved alternating cycles of REFMAC fitting and rebuilding in O. Finally, waters were added using ARP[35]. The substrate-peptide crystals were isomorphous to the recruitment-peptide crystals, and the recruitment-peptide complex was used as the start point for refinement of this structure. The final statistics are given in Table 1.

RECEIVED 12 AUGUST 1999; REVISED 30 SEPTEMBER 1999; ACCEPTED 30 SEPTEMBER 1999; PUBLISHED 14 OCTOBER 1999.

1. Morgan, D. O. Cyclin-dependent kinases: engines, clocks and microprocessors. *Annu. Rev. Cell. Dev. Biol.* **13,** 261–291 (1997).
2. De Bondt, H. L. *et al.* Crystal structure of cyclin dependent kinase 2. *Nature* **363,** 592–602 (1993).
3. Brown, N. R. *et al.* The crystal structure of cyclin A. *Structure* **3,** 1235–1247 (1995).
4. Jeffrey, P. D. *et al.* Mechanism of CDK activation revealed by the structure of a cyclinA-CDK2 complex. *Nature* **376,** 313–320 (1995).
5. Russo, A., Jeffrey, P. D. & Pavletich, N. P. Structural basis of cyclin dependent kinase activation by phosphorylation. *Nature Struct. Biol.* **3,** 696–700 (1996).
6. Brown, N. R. *et al.* Effects of phosphorylation of threonine 160 on cyclin-dependent kinase 2 structure and activity. *J. Biol. Chem.* **274,** 8746–8756 (1999).
7. Songyang, Z. *et al.* Use of an oriented peptide library to determine the optimal substrates of protein kinases. *Curr. Biol.* **4,** 973–982 (1994).
8. Higashi, H. *et al.* Differences in substrate specificity between CDK2-cyclin A and CDK2-cyclin E *in vitro*. *Biochem. Biophys. Res. Commun.* **216,** 520–525 (1995).
9. Holmes, J. K. & Solomon, M. J. A predictive scale for evaluating cyclin depedent kinase substrates. *J. Biol. Chem.* **271,** 25240–25246 (1996).
10. Kitagawa, M. *et al.* The consensus motif for phosphorylation by cyclin D1-CDK4 is different from that for phosphorylation by cyclin A/E-CDK2. *EMBO J.* **15,** 7060–7069 (1996).
11. Zarkowski, T., U, S., Harlow, E. & Mittnacht, S. Monoclonal antibodies for underphosphorylated retinoblastoma protein identify a cell cycle regulated phosphorylation site targeted by CDKs. *Oncogene* **14,** 249–254 (1997).
12. Zhu, L., Harlow, E. & Dynlacht, B. D. p107 uses a p21^{CIP1}-related domain to bind cyclin/cdk2 and regulate interactions with E2F. *Genes Dev.* **9,** 1740–1752 (1995).
13. Adams, P. D. *et al.* Identification of a cyclin-CDK2 recognition motif present in substrates and p21-like cyclin dependent kinase inhibitors. *Mol. Cell Biol.* **16,** 6623–6633 (1996).
14. Chen, J., Saha, P., Kornbluth, S., Dynlacht, B. D. & Dutta, A. Cyclin binding motifs are essential for the function of p21^{cip1}. *Mol. Cell Biol.* **16,** 4673–4682 (1996).
15. Dynlacht, B. D., Moberg, K., Lees, J. A., Harlow, E. & Zhu, L. Specific regulation of E2F family members by cyclin-dependent kinases. *Mol. Cell Biol.* **17,** 3867–3875 (1997).
16. Schulman, B., Lindstrom, D. L. & Harlow, E. Substrate recruitment to cyclin-dependent kinase 2 by a multipurpose docking site on cyclin A. *Proc. Natl Acad. Sci. USA* **95,** 10453–10458 (1998).
17. Adams, P. D. *et al.* Retinoblastoma protein contains a C-terminal motif that targets it for phosphorylation by cyclin-CDK complexes. *Mol. Cell Biol.* **19,** 1068–1080 (1999).
18. Chen, Y.-N. P. *et al.* Selective killing of transformed cells by cyclin/cyclin dependent kinase 2 antagonists. *Proc. Natl Acad. Sci. USA* **96,** 4325–4329 (1999).
19. Nigg, E. A. Targets of cyclin-dependent protein kinases. *Curr. Opin. Cell Biol.* **5,** 187–193 (1993).
20. Sarcevic, B., Lilischkis, R. & Sutherland, R. L. Differential phosphorylation of T-47D human breast cancer cell substrates by D1, D3, E, and A-type cyclin-CDK complexes. *J. Biol. Chem.* **272,** 33327–33337 (1997).
21. Kelly, B. L., Wolfe, K. G. & Roberts, J. M. Identification of a substrate-targeting domain in cyclin E necessary for phosphorylation of the retinoblastoma protein. *Proc. Natl Acad. Sci. USA* **95,** 2535–2540 (1998).
22. Petersen, B. O., Lukas, J., Sorensen, C. S., Bartek, J. & Helin, K. Phosphorylation of mammalian CDC6 by cyclin A/CDK2 regulates its subcellular localisation. *EMBO J.* **18,** 396–410 (1999).
23. Lowe, E. D. *et al.* The crystal structure of a phosphorylase kinase peptide substrate complex: kinase substrate recognition. *EMBO J.* **16,** 6646–6658 (1997).
24. Skamnaki, V. T. *et al.* The catalytic mechanism of phosphorylase kinase probed by mutational studies. *Biochemistry* (in the press).
25. Russo, A. A., Jeffrey, P. D., Patten, A. K., Massague, J. & Pavletich, N. P. Crystal structure of the p27^{KIP1} cyclin-dependent-kinase inhibitor bound to the cyclin A-CDK2 complex. *Nature* **382,** 325–331 (1996).
26. Canagarajah, B. J., Khokhlatchev, A., Cobb, M. H. & Goldsmith, E. J. Activation mechanism of the MAP kinase ERK2 by dual phosphorylation. *Cell* **90,** 859–869 (1997).
27. Solomon, M. J. & Kaldis, P. in *Results and Problems in Cell Differentiation* (ed. Pagano, M.) 79–109 (Springer, New York, 1998).
28. Sharma, P. *et al.* Identification of substrate binding site of cyclin dependent kinase 5. *J. Biol. Chem.* **274,** 9600–9606 (1999).
29. Kobayashi, H. *et al.* Identification of the domains in cyclin A required for binding to, and activation of, p34cdc2 and p32cdk2 protein kinase subunits. *Mol. Biol. Cell.* **3,** 1279–1294 (1992).
30. Schreuder, H. A., Groendijk, H., van der Laan, J. M. & Wierenga, R. K. The transfer of protein crystals from their original mother liquor to a solution with a completely different precipitant. *J. Appl. Cryst.* **21,** 426–429 (1988).
31. Navaza, J. AMoRe: an automated package for molecular replacement. *Acta Crystallogr. A* **50,** 157–163 (1990).
32. Murshudov, G. N., Vagen, A. A. & Dodson, E. J. Refinement of macromolecular structures by the maximum-likelihood method. *Acta Crystallogr. D* **53,** 240–255 (1997).
33. Read, R. J. Improved coefficients for map calculation using partial structures with errors. *Acta Crystallogr. A* **42,** 140–149 (1986).
34. Jones, T. A., Zou, J. Y., Cowan, S. W. & Kjeldgaard, M. Improved method for building models in electron density maps and the location of errors in these models. *Acta Crystallogr. A* **47,** 110–119 (1991).
35. Lamzin, V. S. & Wilson, K. S. Automated refinement of protein models. *Acta Crystallogr. D* **49,** 129–147 (1993).

ACKNOWLEDGEMENTS

We thank N. Hanlon for the GST–CDK2 GST–Cak1 coexpression vector; J. Hayles for the *Schizosaccharomyces pombe* p13^{suc1} peptide; J. Tucker for optimizing the phospho-CDK2 expression; and the beam-line scientists and staff at Elettra, Trieste, and ESRF station ID14 for their support during data collection. This work was supported by the Medical Research Council and the Royal Society.

Correspondence and requests for materials should be addressed to L.N.J. Coordinates have been deposited in Protein DataBank under accession number 1QMZ.

